



Technical Note

A New Analytical Solution for Solving the Smoluchowski Equation Due to Nanoparticle Brownian Coagulation for Non-Self-Preserving System

Mingzhou Yu^{1,2}, Martin Seipenbusch³, Jinghua Yang¹, Hanhui Jin^{4*}

¹ China Jiliang University, Hangzhou 310028, China

² Institute of Earth Environment, Chinese academy of sciences, China

³ Institute for Mechanical processes Engineering and Mechanics, Karlsruhe Institute of Technology, Germany

⁴ Institute of Fluid Engineering, Zhejiang University, China

ABSTRACT

The Smoluchowski equation has become a fundamental equation in nanoparticle processes since it was proposed in 1917, whereas the achievement of its analytical solution remains a challenging issue. In this work, a new analytical solution, which is absolutely different from the conventional asymptotic solutions, is first proposed and verified for non-self-preserving nanoparticle systems in the free molecular regime. The Smoluchowski equation is first converted to the form of moment ordinary differential equations by the performance of Taylor expansion method of moments and subsequently resolved by the separate variable technique. In the derivative, a novel variable, $g = m_0 m_2 / m_1^2$, where m_0 , m_1 and m_2 are the first three moments, is first revealed which can be treated as constant. Three specific models are proposed, two with a constant g (an Analytical Model with Constant g (AMC), and a Modified Analytical Model with Constant g (MAMC)), and another with varying g (a finite Analytical Model with Varying g (AMV)). The AMC model yields significant errors, while its modified version, i.e., the MAMC model, is able to produce highly reliable results. The AMV is verified to have the capability to solve the Smoluchowski equation with the same precision as the numerical method, but an iterative procedure has to be employed in the calculation.

Keywords: Analytical solution; Taylor-expansion method of moments; Smoluchowski equation; Nanoparticle Brownian coagulation; Free molecular regime.

INTRODUCTION

Brownian coagulation is regarded as the most important inter-particle mechanism modifying the size distribution of particles in processes involving nanoparticle synthesis, polymerization, aerosol, emulsification and flocculation (Fox, 2008; Anand *et al.*, 2012; Buesser and Pratsinis, 2012; Menz *et al.*, 2014). Because of Brownian coagulation, the particle systems are always unstable, even in the absence of turbulence (Friedlander, 2000; Crowe *et al.*, 2011; Sitariski, 2012; Wei, 2013). The theory for Brownian coagulation was originally devised for liquids by Smoluchowski (1917) and was subsequently applied in other chemical process and environmental fields. The governing equation for Brownian coagulation has been established for nearly a century in its integral-differential form (Müller, 1928), which is usually called the Smoluchowski equation (SE), but the solution

for it remains a challenging issue due to its nonlinear integral-differential property (Debry *et al.*, 2003; Wang *et al.*, 2007; Wei and Kruis, 2013). Currently, the process of Brownian coagulation receives much more attention in the newly emerging fields of aerosol science, cloud science, supercritical fluid processes and nanoparticle synthesis engineering (Garrick, 2011; Yu and Lin, 2010a; Buesser and Pratsinis, 2012), where the quick and reliable predication of the size distribution of particles has become a critical issue (Seipenbusch *et al.*, 2008). In such conditions, a reliable analytical solution for solving SE due to Brownian coagulation becomes necessary.

The solution for SE due to Brownian coagulation has been widely studied by researchers for many years, including the analytical solution and numerical solution, which have been reviewed in (Kruis *et al.*, 2000; Vogel *et al.*, 2014). Although the numerical solution is better than the analytical solution in precision (Wang *et al.*, 2007; Yuan and Fox, 2011; Zhao and Zheng, 2009; Wei and Kruis, 2013; Menz *et al.*, 2014), it consumes much more computational expenses and thus may not be suited for the quick determination of particle properties (Claudotte *et al.*, 2010; Rigopoulos, 2010).

* Corresponding author.

E-mail address: enejhh@zju.edu.cn; yumz@ieecas.cn

The analytical solution was firstly used to solve the SE due to Brownian coagulation by Smoluchowski (1917), but this work is limited to monodisperse particles. In fact, in the atmospheric and process engineering conditions, most particles are polydisperse, rather than monodisperse (Friedlander, 2000; Kim and Kim, 2002; Khalili *et al.*, 2010; Buesser and Pratsinis, 2012), and the Smoluchowski analytical solution is only an ideal model and cannot be applied in real conditions. In the recent studies on engineered nanoparticle exposure, the Smoluchowski analytical solution was further developed and extended from monodisperse systems to bidisperse systems, but it is still limited to its inability to characterize the evolution of size distributions (Seipenbusch *et al.*, 2008). An analytical method for solving size-resolved coagulation has been developed based on the use of similarity transformation for the size distribution function (Swift and Friedlander, 1964; Friedlander and Wang, 1966). It is determined that the shapes of the distribution at different times are similar when reduced by a scale factor, and the particle must be at the self-preserving status (Swift and Friedlander, 1964). The self-preserving theory is considered to be among the most important theories in particle science in which the geometric standard deviation (GSD) of the size distribution is kept constant, whereas it is inconsistent with the property of some particles because the GSD may be an arbitrary value more than 1.0. Lee and Chen (1984), Lee *et al.* (1984) and Park *et al.* (1999) found that it is feasible to assume the size distribution to follow the log-normal distribution, and based on this assumption, his group successfully developed a series of analytical models for solving SE due to Brownian coagulation at different size regimes. However, as they acknowledged in their works, the formulas for obtaining total particle number concentration, geometric standard deviation or geometric mean diameter have to be coupled and dependent of each other, thus, iterative techniques have to solve the coupled equations.

Since proposed in 2008 (Yu *et al.*, 2008), the Taylor-expansion method of moments (TEMOM) has been widely employed in studies due to its simple mathematical construction of ordinary differential equations and highly reliable precision (Yu and Lin, 2009a, b, 2010b; Xie *et al.*, 2012). It has also been developed in different versions with specific requirements (Lin and Chen, 2013; Chen *et al.*, 2014). Similar to the solution of Lee *et al.* (1984), the asymptotic behavior of the TEMOM ordinary differential equations (TEMOM ODEs) has been investigated in (Xie and Wang, 2013; Xie, 2014). In recent studies on the TEMOM ODEs, a novel variable, $g = m_0 m_2 / m_1^2$, where m_0 , m_1 and m_2 are the first three moments, it was revealed that they can be treated as constant in the derivation; thus, the analytical solution for SE can be directly achieved. In fact, in the studies of the TEMOM ODEs, it was found that the geometric standard deviation of particle number distribution can be characterized by the definition $\ln^2(\sigma_g) = (1/9)\ln(g)$, where σ_g is the GSD of the size distribution, although no log-normal distribution was employed. For GSD, it has been confirmed that it is a constant of 1.345 from the TEMOM method and QMOM method (Yu *et al.*, 2008) and 1.355 from log-normal method (Lee *et al.*, 1984) in the free molecular regime. The variance

of GSD with the Knudsen number is presented in Fig. 1. It needs to emphasize the TEMOM ODEs with three order Taylor expansion series is the best selection for deriving the analytical solution due to its both simple mathematical structure and high precision, which has been discussed in (Yu *et al.*, 2008). The newly proposed solution has been verified with high precision for self-preserving particles, but its ability for non-self-preserving particles still needs to be verified.

Therefore, in this work, an alternative analytical solution for solving SE due to Brownian coagulation will be proposed and verified as the particle deviates from the self-preserving status. The investigated particles are limited to the free molecular regime; thus, the newly proposed solution is only valid with a Knudsen number of more than 10, as shown in Fig. 1. To validate the analytical solution with precision, the numerical method from the highly reliable Runge-Kutta algorithm (NM) for the same ODEs will be used as a reference.

THEORIES

The integral-differential SE was firstly proposed by Müller in 1928 based on the Smoluchowski groundbreaking work for coagulation process (Müller, 1928; Smoluchowski, 1917), and it takes the following form,

$$\frac{\partial n(v, t)}{\partial t} = \frac{1}{2} \int_0^v \beta(v-v', v') n(v-v', t) n(v', t) dv' - n(v, t) \int_0^\infty \beta(v, v') n(v', t) dv' \quad (1)$$

where $n(v, t)dv$ is the particle number whose volume is between v and $v + dv$ at time t , and $\beta(v, v')$ is the collision kernel for two particles of volumes v and v' . In the free molecular regime, the collision kernel was derived from gas kinetic theory, which is expressed by (Friedlander, 2000),

$$\beta(v, v') = B_1 \left(\frac{1}{v} + \frac{1}{v'} \right)^{\frac{1}{2}} \left(\frac{1}{v^{\frac{1}{3}}} + v'^{\frac{1}{3}} \right)^2 \quad (2)$$

where $B_1 = \left(\frac{3}{4\pi} \right)^{\frac{1}{6}} (6k_b T / \rho)^{1/2}$, k_b is the Boltzmann constant, T is the gas temperature and ρ is the mass density of the particles. The Taylor-expansion method of moments (TEMOM) is introduced in solving Eq. (1) with the closure model for the k -th moment (Yu *et al.*, 2008),

$$m_k = \left(\frac{u^{k-2} k^2}{2} - \frac{u^{k-2} k}{2} \right) m_2 + \left(-u^{k-1} k^2 + 2u^{k-1} k \right) m_1 + \left(u^k + \frac{u^k k^2}{2} - \frac{3u^k k}{2} \right) m_0 \quad (3)$$

where u is the Taylor expansion point. In this work, u is defined to be m_1/m_0 . The TEMOM ordinary differential

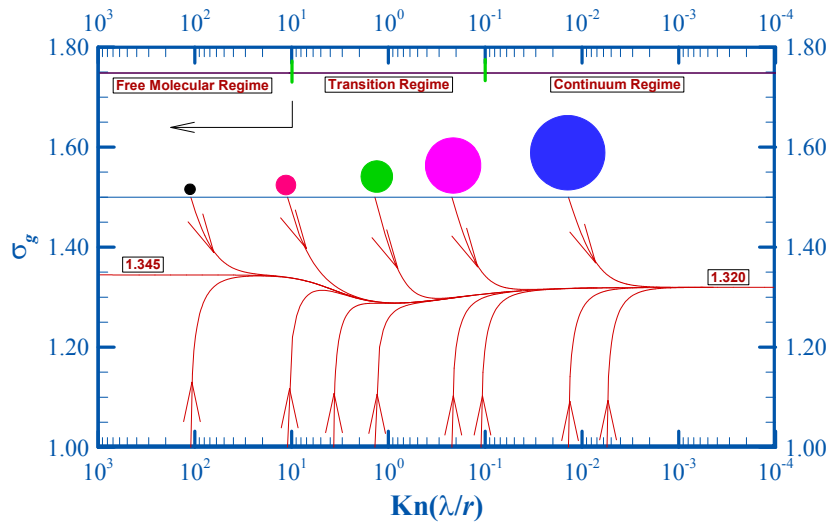


Fig. 1. Changes in the geometric standard deviation (GSD, σ_g) as a function of the Knudsen number (Kn) over the entire size range. λ is the mean free path of gas molecules, 68.410 nm, and r is the particle radius.

equations (TEMOM ODEs) take the following expression (Yu *et al.*, 2011),

$$\begin{cases} \left(\frac{dm_0}{dt}\right)_f = \frac{\sqrt{2}B_1\{65g^2 - 1210g - 9223\}}{5184} m_1(t)^{\frac{1}{6}} m_0(t)^{\frac{11}{6}} \\ \left(\frac{dm_1}{dt}\right)_f = 0 \\ \left(\frac{dm_2}{dt}\right)_f = -\frac{\sqrt{2}B_1\{701g^2 - 4210g - 6859\}}{2592} g^{-\frac{1}{6}} m_1(t)^{\frac{11}{6}} m_2(t)^{\frac{1}{6}} \end{cases} \quad (4)$$

In this equation, $g = m_0 m_2 / m_1^2$, and the k -th moment is defined as $m_k = \int_0^\infty v^k n(v) dv$. The zeroth moment, m_0 , represents the particle number concentration, which decreases with the growth of the particle size. The first moment, m_1 , remains constant in Brownian coagulation process and is proportional to the total particle mass. The second moment, m_2 , is usually used as an index to characterize the total light scattered, which increases with the growth of the particle size and polydispersity (Settumba and Garrick, 2003). If Eq. (4) are further disposed by a dimensionless solution with $m_k = M_k m_{k0}$ and $m_{k0} = N v_{g0}^k$, then they have the following expression,

$$\begin{cases} \left(\frac{dM_0}{d\tau_1}\right)_f = \frac{\sqrt{2}\{65g^2 - 1210g - 9223\}}{5184} M_1(\tau_1)^{\frac{1}{6}} M_0(\tau_1)^{\frac{11}{6}} \\ \left(\frac{dM_1}{d\tau_1}\right)_f = 0 \\ \left(\frac{dM_2}{d\tau_1}\right)_f = -\frac{\sqrt{2}\{701g^2 - 4210g - 6859\}}{2592} g^{-\frac{1}{6}} M_1(\tau_1)^{\frac{11}{6}} M_2(\tau_1)^{\frac{1}{6}} \end{cases} \quad (5)$$

where $\tau_1 = tNB_1(v_{g0})^{1/6}$, and N and v_{g0} are the initial total particle number and geometric mean size, respectively. The same dimensionless time was used in the analytical solution for solving SE with the assumption of a log-normal distribution (Lee *et al.*, 1984). If g can be regarded as a constant, the analytical solutions for Eq. (5) should be,

$$\begin{cases} (M_0(\tau_1))_f = \left(-\frac{5}{6} a_f \tau_1 + M_{00}^{-\frac{5}{6}}\right)^{-\frac{6}{5}} \\ (M_1(\tau_1))_f = M_{10} \\ (M_2(\tau_1))_f = \left(\frac{5}{6} b_f \tau_1 + M_{20}^{\frac{5}{6}}\right)^{\frac{6}{5}} \end{cases} \quad (6)$$

where $a_f = \frac{\sqrt{2}\{65g^2 - 1210g - 9223\}}{5184} M_{10}^{1/6}$ and $b_f = -\frac{\sqrt{2}\{701g^2 - 4210g - 6859\}}{2592} g^{-1/6} M_{10}^{11/6}$. M_{00} , M_{10} and M_{20}

are the zeroth, first and second moments at initial time, separately. In the above derivation, the separation of variables technique was used. Eq. (6) exhibits the novel property in that the first three moments are decoupled, and especially both M_0 and M_2 are only functions of the dimensionless time τ_1 . Here, it needs to point out in the derivation only three order terms of Taylor expansion series are reserved. Although high precision is expected to achieve with higher order terms of Taylor expansion series, it is not feasible here because higher order terms of Taylor expansion series leads to too much complicated TEMOM ODEs whose analytical solution cannot be obtained. In fact, as shown in the following work, three order terms of Taylor expansion series meet the requirement of solving Smoluchowski Equation in precision.

COMPUTATIONS

The calculations were all performed on an Intel (R) Core i7-3573U CPU 2.5 GHz computer with 4GB memory. The fourth order Runge-Kutta method with a fixed time step of 0.001 was used to solve the TEMOM ODEs in the numerical solution. For all numerical and analytical solutions, the total time was up to 100. All the programs codes were written with the C++ Programming language under the platform of Microsoft Visual Studio 2008 compiler. The calculation of the relative error for any variables follows the definition (Yu *et al.*, 2008),

$$RE\% = \frac{\phi - \phi_{NM}}{\phi_{NM}} \times 100\% \tag{7}$$

where ϕ is the arbitrary variable and ϕ_{NM} is the referenced numerical variable. In the present study, a criterion is proposed for assessing the ability of the analytical method in solving SE due to Brownian coagulation, i.e., the investigated analytical method and the reference numerical method are considered to have the same precision in solving SE if the absolute relative errors, $|RE\%|$, are less than 0.050. In the calculation, all initial dimensionless moments take the following expressions:

$$\begin{cases} M_0 = 1 \\ M_1 = \chi \\ M_2 = \chi^4 \end{cases} \tag{8}$$

where $\chi = e^{w_g^2/2}$, $w_g = 3\ln\sigma_{g0}$ and σ_{g0} is the initial GSD. In this work, the determinations of first three moments are reached by three specific models, two with constant GSD (AMC model and MAMC model) and another with varying GSD (AMV model). In the AMC and MAMC, the solutions for the first three moments are decoupled, whereas in the AMV the solutions for the formula, $g = M_0(\tau_1)M_2(\tau_1)/M_1(\tau_1)^2$, as well as for the first three moments, have to be coupled where an iterative calculation is required. In the AMV, g needs to be obtained first with the first three moments at the last time step ($\tau_1 - \Delta t$). It is then used in the acquirement of first three moments at the current time step (τ_1). In this way, the time step size (Δt) should be small enough so that no significant errors arise when introducing g to the solution for M_0 , M_1 and M_2 shown in Eq. (5). In the present study, the time step for the AMV is fixed at 0.001, same as the time step for the NM. Thus, the AMV is actually a finite analytical model.

RESULT AND DISCUSSION

In the free molecular regime, the successful achievement of an analytical solution for the SE is attributed to the novel dynamical property of particles that the GSD of the size distribution can be treated as a constant (Lee *et al.*, 1984; Vemury *et al.*, 1994; Friedlander and Wang, 1966). This treatment is valid for self-preserving particulates since

the GSD in the free molecular has been confirmed to be a constant (Lee *et al.*, 1984). In this work, it needs to be verified whether the newly proposed analytical method can also be valid at the non-self-preserving status, or whether the analytical method is able to produce the result within a reasonable error range for non-self-preserving particles.

The Zero Moment (M_0)

The governing equations for particles dominated solely by Brownian coagulation mechanism must meet the following requirement since the total particle number concentration decreases and the second moment increases with time (Yu *et al.*, 2008),

$$\begin{cases} \left(\frac{dM_0}{d\tau_1}\right)_f < 0 \\ \left(\frac{dM_1}{d\tau_1}\right)_f = 0 \\ \left(\frac{dM_2}{d\tau_1}\right)_f > 0 \end{cases} \tag{9}$$

In the free molecular regime, the effective range of the TEMOM ODEs in terms of GSD is confirmed to be at $\sigma_g \in (1.000, 1.601)$ through solving Eq. (9). In the acquirement of the effective range of GSD, the relationship between σ_g and g , i.e., $\ln^2(\sigma_g) = (1/9)\ln(g)$, is employed. Within this range, the TEMOM model is expected to solve SE due to Brownian coagulation with any initial size distribution. Because the TEMOM ODEs are solved by an analytical solution, the effectiveness needs to be verified by comparison with the existing reliable methods. In the present work, the numerical solution with the highly reliable 4th-order Runge-Kutta algorithm is selected as the reference for comparison (Yu *et al.*, 2008). Figs. 2(a) and 2(b) separately show the $RE\%$ of the AMV and the AMC to the NM for M_0 as the particle initially follows the different distributions, i.e., different initial GSD. The $RE\%$ are obtained through solving Eq. (7) shown in Section 3. Six different initial GSD and σ_{g0} are distributed over the entire effective range of the TEMOM ODEs in terms of GSD. In the performance of the AMC, the GSD is always the same as the initial value, whereas in the AMV, the GSD is updated at the end of each interaction as discussed in Section 3. To make it more convenient to be analyzed, the horizontal axis is scaled by a log operation for Fig. 2(a). The same operation will be executed for Fig. 4(a) below.

Fig. 2(a) shows that the distribution initially deviates much more from the self-preserving size distribution, i.e., σ_{g0} deviates much more from 1.345, which was considered to be the value of the self-preserving status in the free molecular regime (Yu *et al.*, 2008), the absolute value of $RE\%$ achieves larger values. The absolute $RE\%$ s are always limited to a very small range of variance, and they all have the same trend of finally converging to zero for all investigated distributions. The maximum $RE\%$, 0.031, is reached at a distribution with $\sigma_{g0} = 1.600$, once the particle evolves for a

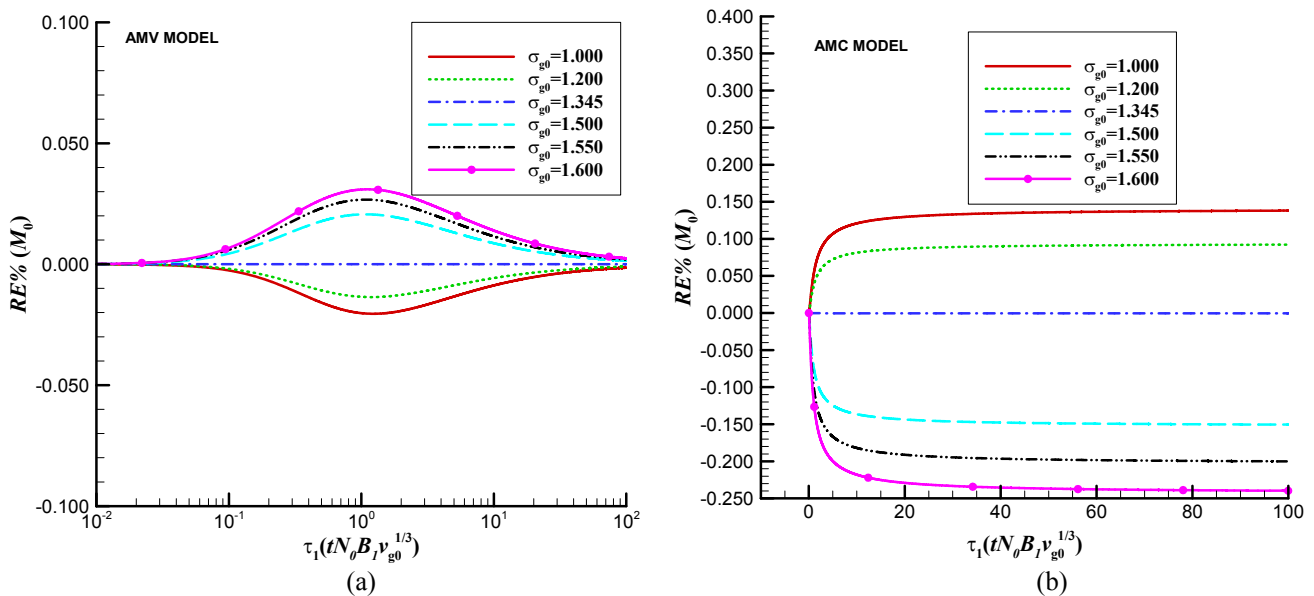


Fig. 2. The comparison of relative errors of the AMV (a) and the AMC (b) to the NM with six different initial size distributions for M_0 .

short dimensionless time, ~ 1.000 . The maximum absolute value of $RE\%$ for each distribution occurs at nearly the same dimensionless time, ~ 1.000 . More importantly, the $RE\%$ for all distributions over the entire evolution time are less than the value of the criterion, 0.050, which is proposed in Section 3. Based on the definition for the criterion shown in Section 3, the AMV can be considered to produce M_0 with the same precision as the NM.

Compared to the AMV, the AMC produces relatively larger errors for M_0 as the same six distributions are investigated, which is clearly shown in Fig. 2(b). In the figure, except for the self-preserving size distribution with $\sigma_{g0} = 1.345$, which is a special case in the free molecular regime (Yu *et al.*, 2008), the absolute values of $RE\%$ for the other distributions are all more than 0.05 once the particles evolve for a short dimensionless time, i.e., ~ 1.000 . It is clear that as the initial GSD deviates much more from 1.345, the larger absolute values of $RE\%$ are generated, which is the same as the AMV shown in Fig. 2(a). In Fig. 2(b), the $RE\%$ approaches 0.250 in the distribution with $\sigma_{g0} = 1.600$. In such a case, the results generated by the AMC cannot be used as reliable results for solving SE due to Brownian coagulation. However, a novel property of the AMC is revealed in Fig. 2(b), in that for any distribution, the value of $RE\%$ quickly approaches its maximum or minimum value at the initial stage (the dimensionless time is below ~ 10.000) and then maintains this value at the later stage, which means the relative errors of the AMC to the NM for producing M_0 are unchanged once the particle evolves for a short time. More importantly, this difference depends only on one quantity, i.e., the initial GSD. Therefore, the modification of the AMC can be achieved by including an additional term accounting for the relative errors of the AMC to the NM. To achieve this, the relationship between the $RE\%$ of the AMC to the NM and the initial GSD for different distributions needs to be determined.

To determine the relationship between the initial GSD

and the $RE\%$, many more initial distributions up to 24 are investigated by the performance of the NM calculation and the AMC calculation. The $RE\%$ of the AMC to the NM relevant to the initial GSD are shown in Fig. 3. The data for the initial GSD, as well as the corresponding $RE\%$, have been attached online as Data-Fig. 3. It shows that the variance of $RE\%$ for M_0 is limited in the range from -0.240 to 0.138. The relationship between the initial GSD and $RE\%$ can be represented by a suitable mathematical equation by performing the 6th degree polynomial fitting technique. In mathematics, the fitting function fits much more to the initial data if the polynomial degree is selected as a larger value. Here, the mathematical equation relating the initial GSD to $RE\%$ is,

$$f(\sigma_{g0})_{\text{free-m0}} = 0.00018895\omega^6 + 0.001492\omega^5 + 0.0043408\omega^4 + 0.0046002\omega^3 - 0.031742\omega^2 - 0.13938\omega - 0.012157 \quad (10)$$

with $\omega = (\sigma_{g0} - 1.359) / 0.16273$. $f(\sigma_{g0})_{\text{free-m0}}$ is the function of σ_{g0} representing the relationship between the initial GSD and the $RE\%$ over the entire effective regime of TEMOM ODEs. Correspondingly, the residuals in the performance of curve fitting are also shown in Fig. 3, whose absolute values are always less than 0.0001, indicating that the fitting Eq. (10) is high reliable. Therefore, the analytical solution for M_0 in Eq. (3) can be modified as following,

$$(M_0(\tau_1))_f = \frac{\left(-\frac{5}{6}a_f\tau_1 + M_{00}\right)^{-\frac{5}{6}}}{1 + f(\sigma_{g0})_{\text{free-m0}}} \quad (11)$$

The Second Moment (M_2)

The second moment, M_2 , is an important quantity

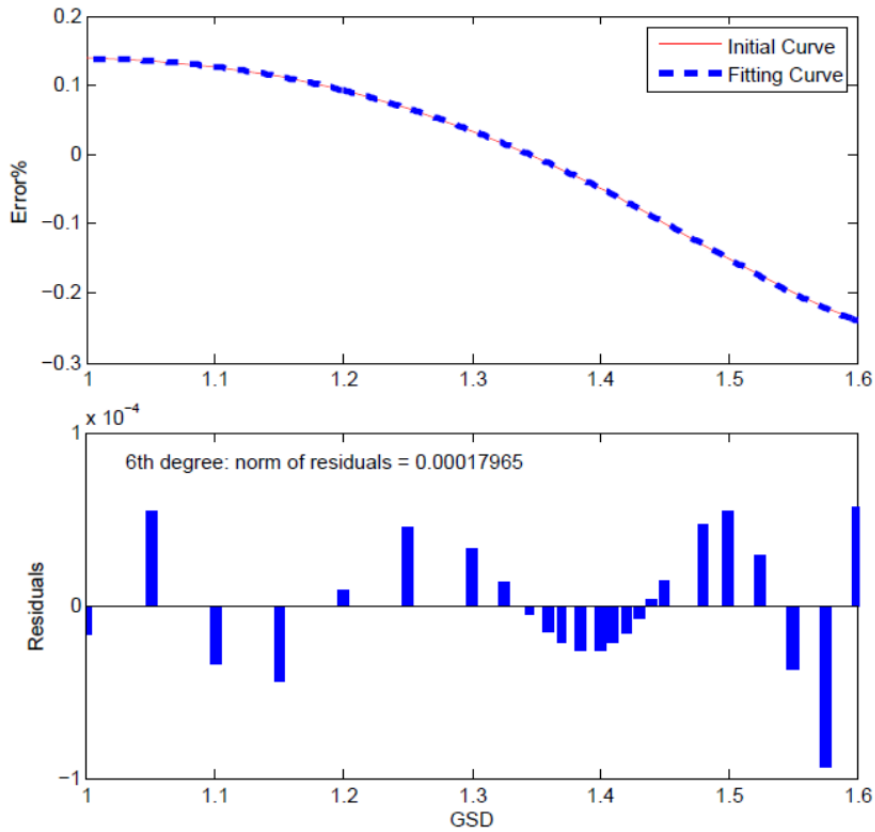


Fig. 3. The $RE\%$ of the AMC to the NM for M_0 relevant to the initial GSD, as well as the corresponding fitting curve, $f(\sigma_{g0})_{free-m0}$ (a); the residuals produced in the performance of the 6-th degree polynomial fitting operation (b).

characterizing particle polydispersity and particle mean size (Friedlander, 2000). Because only the Brownian coagulation mechanism is involved, the second moment always increases with the growth of the particle size and polydispersity (Settumba and Garrick, 2003). In this section, the same six distributions as in Section 4.1 are selected and investigated. The $RE\%$ of the AMV and the AMC to the NM for M_2 are shown in Figs. 4(a) and 4(b), respectively. In Fig. 4(a), the absolute $RE\%$ for all distributions initially increases to each maximum value and then quickly decreases and converges to zero. The lag times to reach the maximum value for all distributions are nearly the same, ~ 1.000 . Over the entire time range, the distribution with the initial GSD deviating more from the self-preserving value of 1.345 has larger $RE\%$. The absolute $RE\%$, 0.069, is achieved in its maximum value at the distribution with $\sigma_{g0} = 1.600$ and at dimensionless time, ~ 1.000 , but it quickly decreases to be less than the value of criterion at the dimensionless time of ~ 1.855 . This means that under the criterion, the AMV is able to produce M_2 with the same precision as the NM once the particle evolves for a short time.

The $RE\%$ of the AMC to the NM for M_2 are shown in Fig. 4(b). In this figure, the $RE\%$ quickly increases to a constant at dimensionless time of ~ 10.000 and later remains at this value at the later stage for all six distributions. This is similar to the zeroth moment shown in Fig. 2(b). An important conclusion can be drawn that the $RE\%$ of the AMC to the NM for M_2 are also unchanged once the

particle evolves for a short time. Therefore, it is feasible to obtain the relationship between the initial GSD and the $RE\%$ for M_2 , which is shown in Fig. 5. The curve obtained by performing the 7th degree polynomial fitting technique, as well as the corresponding residuals, are also shown in this figure. The data for the initial GSD and the corresponding $RE\%$ have been attached online as Data-Fig. 5. The residuals are always below 0.010, ensuring that the fitting equation is reliable, although it is not as high as in Fig. 3 in precision. Here, the fitting equation obtained by the performance of the fitting technique is,

$$f(\sigma_{g0})_{free-m2} = 0.0037563\epsilon^7 + 0.010874\epsilon^6 - 0.016636\epsilon^5 - 0.088877\epsilon^4 - 0.12637\epsilon^3 - 0.10002\epsilon^2 + 0.0075218\epsilon - 0.00032143 \quad (12)$$

with $\epsilon = (\sigma_{g0} - 1.359)/0.16273$. When Eq. (12) is introduced in the solution for M_2 shown in Eq. (6), the modified solution should be,

$$(M_2(\tau_1))_f = \frac{\left(\frac{5}{6}b_f\tau_1 + M_{20}^{\frac{5}{6}}\right)^6}{1 + f(\sigma_{g0})_{free-m2}} \quad (13)$$

Finally, the modified AMC, i.e., the MAMC, takes the following expression,

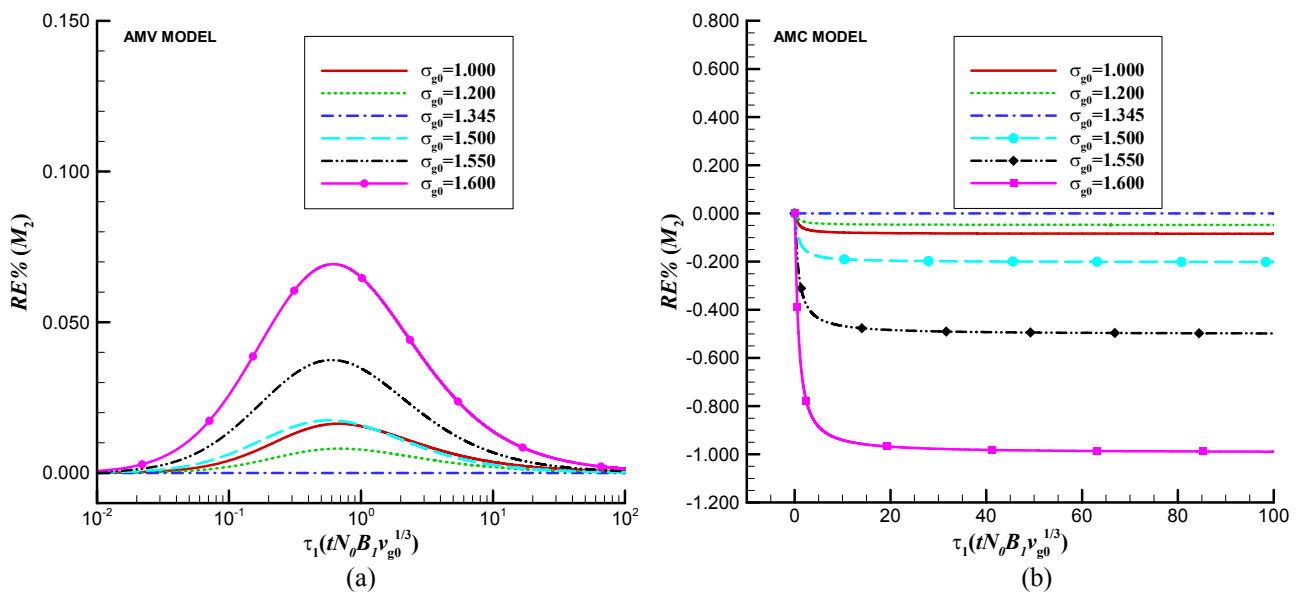


Fig. 4. The comparison of the relative errors of the AMV (a) and the AMC (b) to the NM with six different initial size distributions for M_2 .

$$\left\{ \begin{array}{l} (M_0(\tau_1))_f = \frac{\left(-\frac{5}{6}a_f\tau_1 + M_{00}^{-\frac{5}{6}}\right)^{-\frac{6}{5}}}{1 + f(\sigma_{g0})_{\text{free}-m_0}} \\ (M_1(\tau_1))_f = M_{10} \\ (M_2(\tau_1))_f = \frac{\left(\frac{5}{6}b_f\tau_1 + M_{20}^{\frac{5}{6}}\right)^{\frac{6}{5}}}{1 + f(\sigma_{g0})_{\text{free}-m_2}} \end{array} \right. \quad (14)$$

The MAMC shown in Eq. (14) reserves the advantage of its original version in the decoupled solution for the first three moments, but it generates more precise results because of the additional modified terms accounting for the difference between the original AMC and the NM. Once the first moments are achieved by solving Eq. (14), the key quantities of any particle including the total particle number concentration, the total particle volume concentration, the geometric mean size, and the geometric standard deviation of size distribution, are also determined (Lee and Chen, 1984; Settumba and Garrick, 2003; Yu *et al.*, 2008).

Evolution of the Size Distribution Relevant to the AMV

The GSD is the most important index characterizing the polydisperse property of particles (Lee *et al.*, 1984), and thus, the ability to exactly trace the evolution of GSD with time is the criteria to distinguish good and bad models (Pratsinis, 1988). Figs. 6(a) and 6(b) separately show the varied GSD with time for both AMV and NM, as well as the corresponding $RE\%$ of the AMV to the NM. It is found from Fig. 6(a) that the GSD from the AMV are nearly the same as the NM, although the NM is calculated by fourth order Runge-Kutta interactions, consuming a relatively higher computational

cost. For the four investigated distributions shown in Fig. 6(a), the GSDs are found to quickly converge to a constant, which is consistent with the self-preserving theory first found by Friedlander and Wang (1966) and later confirmed in Lee *et al.* (1984) and Yu *et al.* (2008). In Fig. 6(b), similar to the solution for both M_0 and M_2 shown in Figs. 2(b) and 3(b), the $RE\%$ of the AMV to the NM for GSD are calculated by solving Eq. (7). The variance of $RE\%$ for GSD with time has the same trend as M_0 and M_2 . The absolute $RE\%$ initially increases to approach the maximum and then decreases until it converges to zero. All distributions achieve their own maximum value for GSD at nearly the same time, ~ 1.000 , which is consistent with that for M_0 and M_2 shown in Figs. 2(a) and 4(a). It is also shown the $RE\%$ s for GSD are limited to a very small range of variance with the maximum of 0.015, which is less than the value of criterion proposed in this work shown in Section 3. The AMV is thus verified to be able to characterize the GSD with the same precision as the NM.

Based on the above analysis of the three key statistical quantities, i.e., M_0 , M_2 and σ_g , the AMV is verified to be able to solve SE due to Brownian coagulation for non-self-preserving particles. Thus it has strong potential to replace the NM due to the inherent advantage of the analytical solution.

Verification of the MAMC Model

In Sections 4.1 and 4.2, the MAMC has been proposed as the modified version of the AMC, but its ability for solving SE due to Brownian coagulation needs to be verified quantitatively. To validate the MAMC, the NM is selected to be the reference for comparison. In Fig. 7, the comparison of the results produced by the NM, the MAMC and the AMC for M_0 , M_2 and σ_g is exhibited. As examples, two different initial distributions, i.e., $\sigma_{g0} = 1.200$ and 1.500, are selected. For both M_0 and M_2 , it is shown that the results

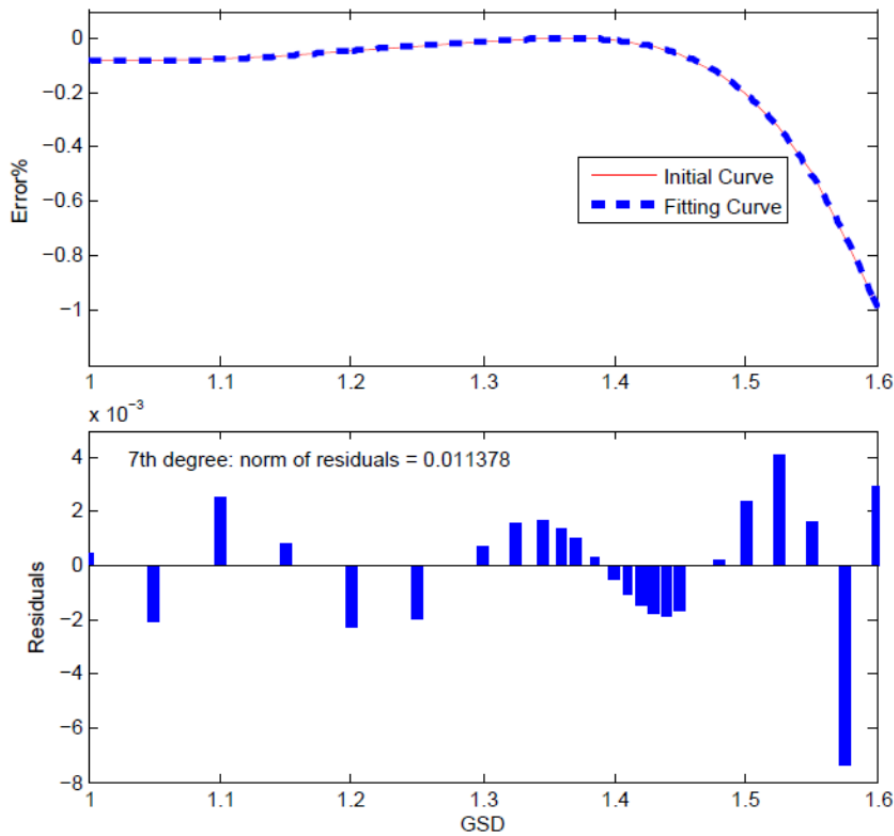


Fig. 5. The $RE\%$ of the AMC to the NM for M_2 relevant to the initial GSD, as well as the corresponding fitting curve, $f(\sigma_{g0})_{free-m0}$ (a); the residuals produced in the performance of the 7th degree polynomial fitting operation (b).

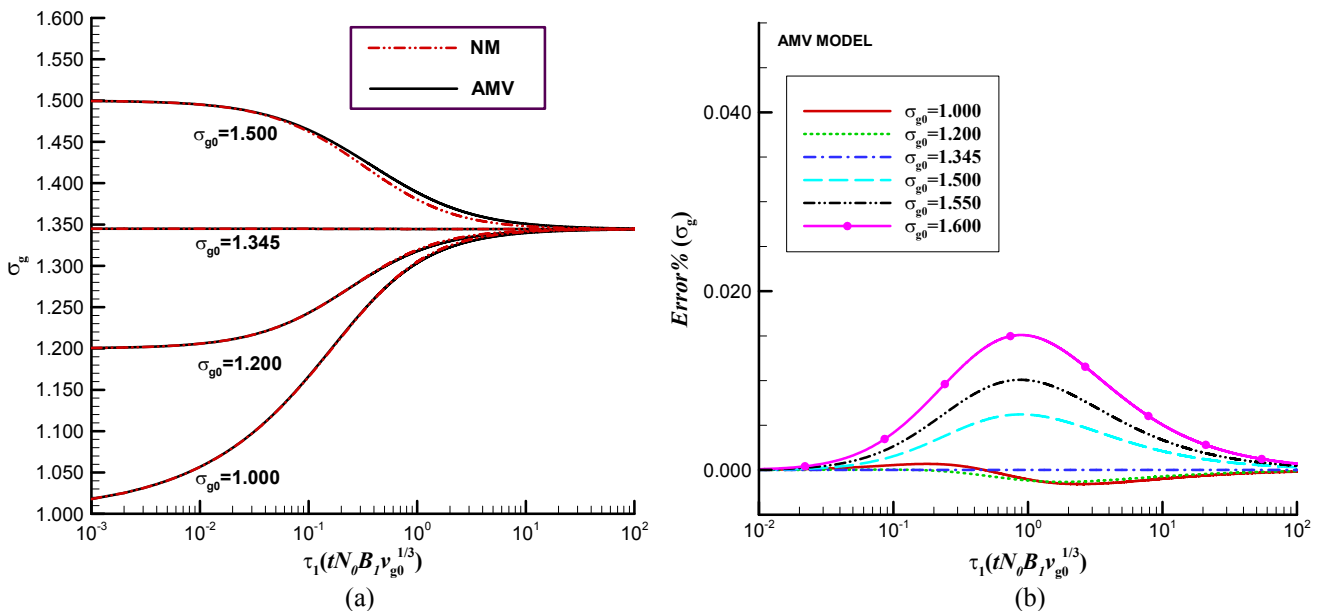


Fig. 6. The comparison of GSD produced by the NM and the AMV with time (a) and the $RE\%$ of the AMV to the NM (b).

from the MAMC quickly converge to the NM as the particle evolves for dimensionless time, $\sim 10,000$, whereas the AMC deviates clearly from the NM. For GSD, the MAMC also converges to the NM after the same time. For the two investigated initial distributions, the GSDs are found to

converge to the same value, 1.345, which is also the value of a particle system dominated by Brownian coagulation with the self-preserving size distribution status (Yu *et al.*, 2008).

To verify whether the MAMC has the ability to solve SE due to Brownian coagulation over the entire effective GSD

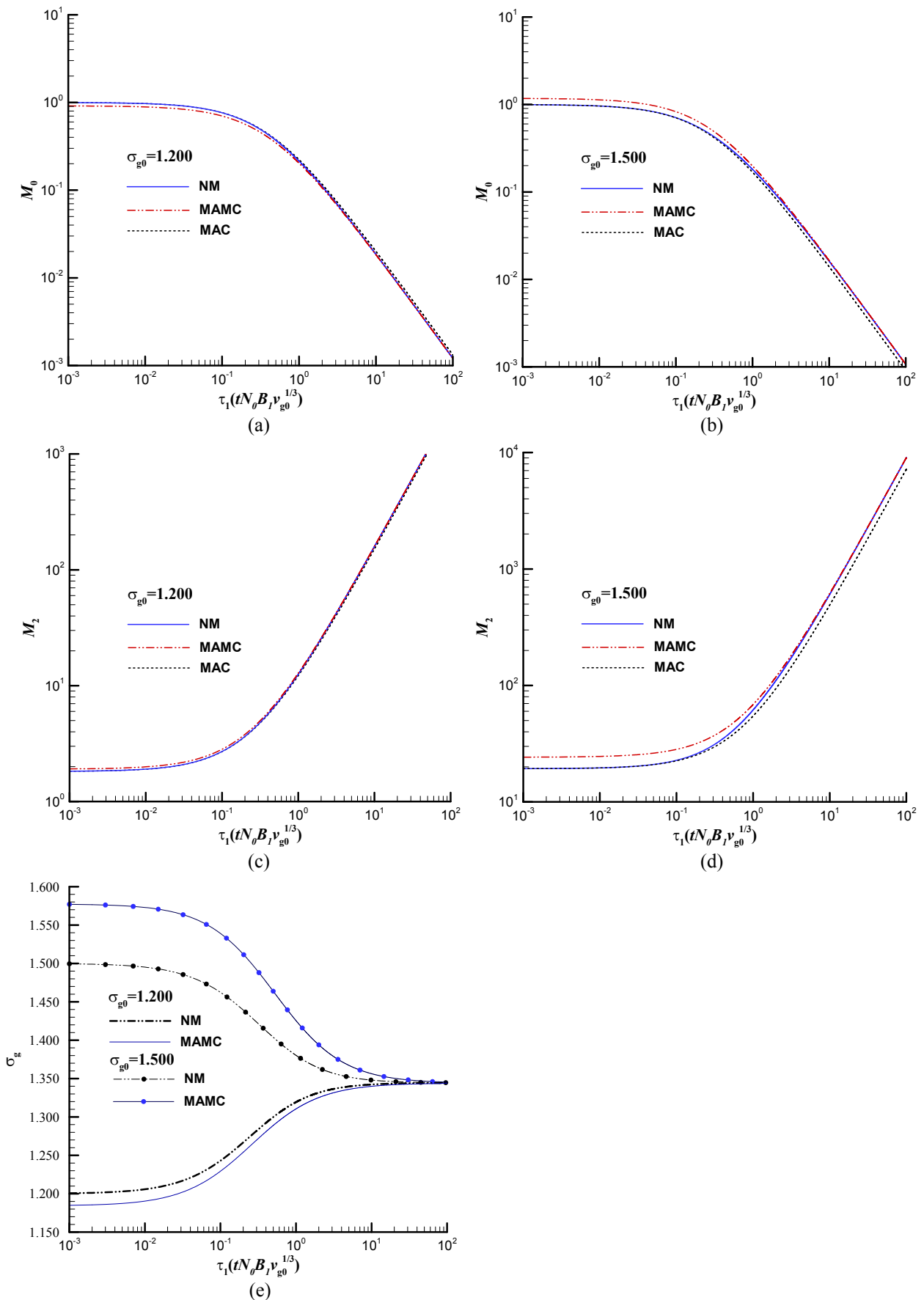


Fig. 7. The variance of M_0 with $\sigma_{g0} = 1.200$ (a), 1.500 (b), M_2 with $\sigma_{g0} = 1.200$ (c), 1.500 (d) and GSD (e) with time up to $\tau_1 = 100$.

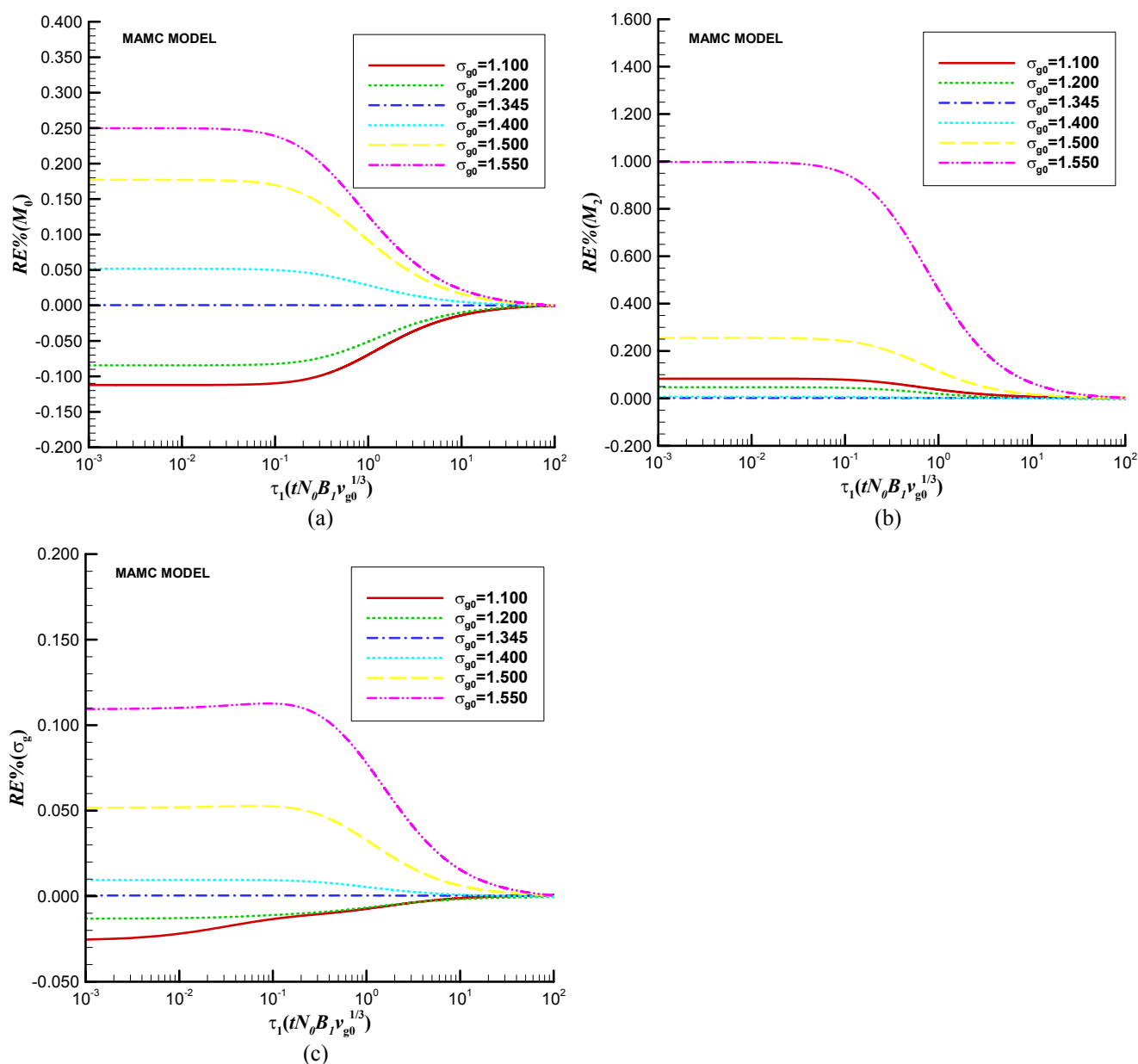


Fig. 8. The $RE\%$ of the MAMC to the NM for M_0 (a), M_2 (b) and σ_g (c) with different initial distributions.

range, many more distributions are required to be investigated and tested. To achieve this, six representative distributions, which span the entire effective GSD range, are selected. The $RE\%$ s of the MAMC to the NM for M_0 , M_2 and σ_g with time are obtained by solving Eq. (7) and are presented in Fig. 8. For all six representative distributions, the variances of $RE\%$ for M_0 , M_2 and σ_g with time exhibit the same trend, and ultimately, they all converge to zero. This result indicates that the differences between the NM and MAMC for the above three key statistical quantities, i.e., M_0 , M_2 and σ_g , decrease with time until the difference vanishes. In the figure, the absolute values of $RE\%$ for M_0 , M_2 and σ_g for each distribution are less than the criterion value, 0.050, once the dimensionless time of evolution is more than ~ 10.000 . In addition, it is found that the closer to 1.345 the GSD is the less lag time it takes to approach the criterion.

In fact, the dimensionless time, $\tau_1 = 10.000$, corresponds to the physical time, $t = 1.115 \times 10^{-3}$ s, under the conditions in Section 3. In such a case, an important conclusion can be drawn that the MAMC has the same capability to solve SE due to Brownian coagulation as the NM once the particle evolves for a very short time. For longer times of evolution, there is higher precision of the MAMC. The MAMC has a significant advantage because it does not require interactive calculation and, more importantly, the requirement of moments is decoupled. In conclusion, the MAMC has potential to replace the NM in processes involving Brownian coagulation due to its superior properties, and therefore, it is regarded as the ideal analytical solution for solving SE due to Brownian coagulation.

CONCLUSIONS

An analytical solution for the Smoluchowski equation (SE) is proposed and verified for resolving the Brownian coagulation process of non-self-preserving nanoparticle systems in the free molecular regime. The concept and approach employed in this study are simple and straightforward. The newly proposed analytical solution is absolutely different from the existing asymptotic solutions, and it is expected to extend beyond the asymptotic solution in its scope of application.

The novel property of coagulated systems that the geometric standard deviation (GSD) of the size distribution can be treated as constant is employed in the derivation. In the performance of the analytical solutions, three specific models, i.e., the analytical model with constant geometric standard deviation (AMC model), the analytical model with varying geometric standard deviation (AMV model), and the improved version of the AMC (MAMC model), are separately proposed and verified by comparison with a highly reliable method, i.e., the numerical method with the 4th-order Runge-Kutta algorithm (NM). The AMV is verified to have the capability to solve SE due to Brownian coagulation for non-self-preserving systems with the same precision as the NM under the criterion proposed in this work, but the solutions for the first three moments, as well as the novel variable, $g = M_0(\tau_1)M_2(\tau_1)/M_1(\tau_1)^2$, have to be coupled and needs iterative calculation. The AMC yields significant errors for M_0 , M_2 and σ_g that cannot be ignored; thus, it is unsuitable for solving SE due to Brownian coagulation at non-self-preserving status. The MAMC reserves the advantage of the AMC in the decoupled solution for moments and is verified to produce the same results as the NM under the criterion after the particle evolves for a notably short dimensionless time $\tau_1 = \sim 10.000$, and thus has strong potential to replace the numerical method in the field of particle processes.

ACKNOWLEDGMENTS

Dr. Yu would like to thank the Alexander von Humboldt Foundation with No. 1136169 and Open foundation of State Key Laboratory of Loess and Quaternary Geology for financial support. The authors would also like to thank the joint support of the National Natural Science Foundation of China with No. 11372299, No. 11132008, Sino-German Foundation with No. GZ971, and ZJNSFC with No. LQ12A05001 and LY13E080007.

SUPPLEMENTARY MATERIALS

Supplementary data associated with this article can be found in the online version at <http://www.aaqr.org>.

REFERENCES

- Anand, S., Mayya, Y.S., Yu, M., Seipenbusch, M. and Kasper, G. (2012). A Numerical Study of Coagulation of Nanoparticle Aerosols Injected Continuously into a Large, Well Stirred Chamber. *J. Aerosol Sci.* 52: 18–32.
- Buesser, B. and Pratsinis, S.E. (2012). Design of Nanomaterial Synthesis by Aerosol processes. *Annu. Rev. Chem. Biomol. Eng.* 3: 103–127.
- Chen, Z., Lin, J. and Yu, M. (2014). Direct expansion Method of Moments for Nanoparticle Brownian Coagulation in the Entire Size Regime. *J. Aerosol Sci.* 67: 28–37.
- Claudotte, L., Rimbart, N. and Gardin, P. (2010). A Multi-QMOM Framework to Describe Multi-component Agglomerates in Liquid Steel. *AIChE J.* 56, 2347–2355.
- Crowe, C.T., Sommerfeld, M. and Tsuji, Y. (2011). *Multiphase Flows with Droplets and Particles*, CRC Press New York, CRC Press.
- Debry, E., Sportisse, B. and Jourdain, B. (2003). A Stochastic Approach for the Numerical Simulation of the General Dynamics Equation for Aerosols. *J. Comput. Phys.* 184: 649–669.
- Fox, R.O. (2008). A Quadrature-based Third-order moment Method for Dilute Gas-particle Flows. *J. Comput. Phys.* 227: 6313–6350.
- Friedlander, S.K. and Wang, C.S. (1966). The Self-preserving Particle Size Distribution for Coagulation by Brownian Motion. *J. Colloid Interface Sci.* 22: 126–132.
- Friedlander, S.K. (2000). *Smoke, Dust and Haze: Fundamentals of Aerosol Behavior*, 2nd ed, New York WileyInterscience 1977333 p. John Wiley & Sons, Inc.
- Garrick, S.C. (2011). Effects of Turbulent Fluctuations on Nanoparticle Coagulation in Shear Flows. *Aerosol Sci. Technol.* 45: 1272–1285.
- Khalili, S., Lin, Y., Armaou, A. and Matsoukas, T. (2010). Constant Number Monte Carlo Simulation of Population Balances with Multiple Growth Mechanisms. *AIChE J.* 56: 3137–3145.
- Kim, D.J. and Kim, K.S. (2002). Analysis on Nanoparticle Growth by Coagulation in Silane Plasma Reactor. *AIChE J.* 48: 2499–2509.
- Kruis, F.E., Maisels, A. and Fissan, H. (2000). Direct Simulation Monte Carlo Method for Particle Coagulation and Aggregation. *AIChE J.* 46: 1735–1742.
- Lee, K.W. and Chen, H. (1984). Coagulation Rate of Polydisperse Particles. *Aerosol Sci. Technol.* 3: 327–334.
- Lee, K.W., Chen, H. and Gieseke, J.A. (1984). Log-Normally Preserving Size Distribution for Brownian Coagulation in the Free-Molecule Regime. *Aerosol Sci. Technol.* 3: 53–62.
- Lin, J. and Chen, Z. (2013). A Modified TEMOM Model for Brownian Coagulation of Nanoparticles Based on the Asymptotic Solution of the Sectional Method. *Sci. China Technol. Sci.* 56: 3081–3092.
- Menz, W.J., Akroyd, J. and Kraft, M. (2014). Stochastic Solution of Population Balance Equations for Reactor Networks. *J. Comput. Phys.* 256, 615–629.
- Müller, H. (1928). Zur Allgemeinen Theorie der Raschen Koagulation. *Kolloidchem. Beih.* 27: 223–250.
- Park, S., Lee, K., Otto, E. and Fissan, H. (1999). Log-normal Size Distribution Theory of Brownian Aerosol Coagulation for the Entire Particle Size Range: Part I—Analytical Solution Using the Harmonic Mean Coagulation. *J. Aerosol Sci.* 30: 3–16.
- Pratsinis, S. (1988). Simultaneous Nucleation, Condensation, and Coagulation in Aerosol Reactors. *J. Colloid Interface*

- Sci.* 124, 416–427.
- Rigopoulos, S. (2010). Population Balance Modelling of Polydispersed Particles in Reactive Flows. *Prog. Energy Combust. Sci.* 36: 412–443.
- Seipenbusch, M., Binder, A. and Kasper, G. (2008). Temporal Evolution of Nanoparticle Aerosols in Workplace Exposure. *Ann. Occup. Hyg.* 52: 707–716.
- Settumba, N. and Garrick, S.C. (2003). Direct Numerical Simulation of Nanoparticle Coagulation in a Temporal Mixing Layer via a Moment Method. *J. Aerosol Sci.* 34: 149–167.
- Sitariski, M.A. (2012). Brownian Coagulation of Knudsen Particles on Evaporating/Condensing Aerosol Droplet; Modeling of Capture of Soot Particles by Marine Fog. *Aerosol Air Qual. Res.* 12: 1189–1199.
- Smoluchowski, M. (1917). Versuch einer Mathematischen Theorie der Koagulationskinetik Kolloider. *Z. Phys. Chem.* 92: 129–168.
- Swift, D.L. and Friedlander, S.K. (1964). The Coagulation of Hydrosols by Brownian Motion and Laminar Shear Flow. *J. Colloid Sci.* 19: 621–647.
- Vemury, S., Kusters, K. and Pratsinis, S. (1994). Time-lag for Attainment of the Self-preserving Particle Size Distribution by Coagulation. *J. Colloid Interface Sci.* 165: 53–59.
- Vogel, U., Savolainen, K., Wu, Q., van Tongeren, M., Brouwer, D. and Berges, M. (2014). *Handbook of Nanosafety: Measurement, Exposure and Toxicology*, Elsevier.
- Wang, L.P., Xue, Y. and Grabowski, W.W. (2007). A Bin Integral Method for Solving the Kinetic Collection Equation. *J. Comput. Phys.* 226: 59–88.
- Wei, J. (2013). A Fast Monte Carlo Method Based on an Acceptance-Rejection Scheme for Particle Coagulation. *Aerosol Air Qual. Res.* 13: 1273–1281.
- Wei, J. and Kruijs, F.E. (2013). GPU-accelerated Monte Carlo Simulation of Particle Coagulation Based on the Inverse Method. *J. Comput. Phys.* 249: 67–79.
- Xie, M.L., Yu, M.Z. and Wang, L.P. (2012). A TEMOM Model to Simulate Nanoparticle Growth in the Temporal Mixing Layer Due to Brownian Coagulation. *J. Aerosol Sci.* 54: 32–48.
- Xie, M.L. and Wang, L.P. (2013). Asymptotic Solution of Population Balance Equation Based on TEMOM Model. *Chem. Eng. Sci.* 94: 79–83.
- Xie, M.L. (2014). Asymptotic Behavior of TEMOM Model for Particle Population Balance equation over the Entire Particle Size Regimes. *J. Aerosol Sci.* 67: 157–165.
- Yu, M., Lin, J. and Chan, T. (2008). A New Moment Method for Solving the Coagulation Equation for Particles in Brownian Motion. *Aerosol Sci. Technol.* 42: 705–713.
- Yu, M. and Lin, J. (2009a). Solution of the Agglomerate Brownian Coagulation Using Taylor-expansion Moment Method. *J. Colloid Interface Sci.* 336: 142–149.
- Yu, M. and Lin, J. (2009b). Taylor-expansion Moment Method For agglomerate Coagulation Due to Brownian Motion in the Entire Size Regime. *J. Aerosol Sci.* 40: 549–562.
- Yu, M. and Lin, J. (2010a). Nanoparticle-laden Flows via Moment Method: A Review. *Int. J. Multiphase Flow* 36: 144–151.
- Yu, M. and Lin, J. (2010b). Binary Homogeneous Nucleation and Growth of Water-sulfuric Acid Nanoparticles Using a TEMOM Model. *Int. J. Heat Mass Transfer* 53: 635–644.
- Yu, M., Lin, J., Jin, H. and Jiang, Y. (2011). The Verification of the Taylor-expansion Moment Method for the Nanoparticle Coagulation in the Entire Size Regime Due to Brownian Motion. *J. Nanopart. Res.* 13: 2007–2020.
- Yuan, C. and Fox, R.O. (2011). Conditional Quadrature Method of Moments for Kinetic Equations. *J. Comput. Phys.* 230: 8216–8246.
- Zhao, H. and Zheng, C. (2009). A New Event-driven Constant-volume Method for Solution of the Time Evolution of Particle Size Distribution. *J. Comput. Phys.* 228: 1412–1428.

Received for review, March 6, 2014
Accepted, July 22, 2014

Supplementary Materials

Data for Fig. 3

1.000	0.138075E+00
1.050	0.135069E+00
1.100	0.126370E+00
1.150	0.112136E+00
1.200	0.922143E-01
1.250	0.662892E-01
1.300	0.340544E-01
1.325	0.155252E-01
1.345	-0.442702E-03
1.360	-0.130650E-01
1.370	-0.217797E-01
1.385	-0.352782E-01
1.400	-0.492604E-01
1.410	-0.588290E-01
1.420	-0.685799E-01
1.430	-0.784944E-01
1.440	-0.885532E-01
1.450	-0.987351E-01
1.480	-0.129748E+00
1.500	-0.150492E+00
1.525	-0.175931E+00
1.550	-0.200055E+00
1.575	-0.221797E+00
1.600	-0.239713E+00

Data for Fig. 5

1.000	-0.839793E-01
1.050	-0.815256E-01
1.100	-0.744301E-01
1.150	-0.629307E-01
1.200	-0.474195E-01
1.250	-0.290733E-01
1.300	-0.108808E-01
1.325	-0.367745E-02
1.345	0.690769E-04
1.360	0.111915E-02
1.370	0.719954E-03
1.385	-0.194752E-02
1.400	-0.769415E-02
1.410	-0.136214E-01
1.420	-0.215375E-01
1.430	-0.317468E-01
1.440	-0.445890E-01
1.450	-0.604426E-01
1.480	-0.130492E+00
1.500	-0.201145E+00
1.525	-0.325020E+00
1.550	-0.498085E+00
1.575	-0.727468E+00
1.600	-0.989177E+00